CrossMark
click for updates

A DFT study of the adsorption of O_2 and H_2O on Al(111) surfaces

Xin Wei,[a] Chaofang Dong,*[a] Zhanghua Chen,[b] Kui Xiao[a] and Xiaogang Li[a]

Using first-principles calculations that are based on density functional theory, the molecular and dissociative adsorptions of O_2 and H_2O on a clean and O pre-adsorbed Al(111) surface were systematically investigated. The van der Waals dispersion correction is considered for the molecular adsorption of H_2O. We found that O_2 dissociates into O atoms which can adsorb on fcc and hcp sites. The stability ranking for O atoms on the clean Al(111) surface is fcc > hcp. The energy barriers for the migration of a single O atom from a hcp to a fcc site on a clean and O pre-adsorbed Al(111) surface are 25.91 kJ mol^{-1} and 28.67 kJ mol^{-1}, respectively, which means that the pre-adsorbed O atom inhibits the migration of O atoms on the surface. H_2O molecules cannot dissociate on both clean and O pre-adsorbed Al(111) surfaces spontaneously. The pre-adsorbed O atom can strengthen the adsorption of H_2O and promote its deformation. The dissociation adsorption of H_2O, that is, the co-adsorption of OH and H, is much stronger than the molecular H_2O adsorption. The energy barrier of H_2O dissociation is 137.58 kJ mol^{-1} on a clean Al(111) surface, however, it decreases to 38.18 kJ mol^{-1} with the aid of a pre-adsorbed O atom, suggesting that a pre-adsorbed O atom can promote the dehydrogenation reaction of H_2O.

1. Introduction

Understanding the interaction of gas molecules (O_2 and H_2O) with metal surfaces is critically important for many applications such as corrosion. Aluminum and its alloys are widely used outdoors[1–6] because of their excellent mechanical properties and corrosion resistance. It has been shown that corrosion products play an important role in their corrosion resistance.[7] The adsorption and reaction of O_2 and H_2O on metal surfaces is crucial to the formation of oxide films. Because of the absence of d-electrons and a simple geometrical structure, a gas/Al system is simpler than transition metals. As mentioned by Leygraf and Graedel,[8] the time scale for surface film formation is approximately one microsecond, which means it occurs too fast to be observed or detected by experiments. Thus, theoretical calculations must be used to investigate the mechanism of the gas adsorption.

The oxidation process is a key step of dissociative adsorption of O_2 on the surface. To gain some insights into the mechanism of the oxidation of Al surfaces, O_2 adsorption on Al(111) surfaces has been studied experimentally and theoretically by researchers.[9–18] Pashutski *et al.*[9] studied the adsorption of O_2 on Al(100) at 80 K using Auger and X-ray photoelectron

spectroscopy. The results showed that Al_xO_y oxides were formed in $x : y$ ratios from 3 : 1 to 1 : 1 at low coverage, and the oxide layer transformed to the familiar Al_2O_3 at higher coverage or upon heating to room temperature. Experiments clearly indicate a mysteriously large number of adsorbed single oxygen atoms instead of pairs.[10,11] The calculation results show that O_2 can adsorb on multiple original sites on the Al(111) surface.[12,13] Experiments and theoretical calculations support chemisorption only on the fcc site of the first layer of Al(111),[14,15] and O_2 does not penetrate into subsurface sites.[16] Liu *et al.*[17] predicted that O_2 molecule can be adsorbed on the Al(111) surface with a barrier of approximately 0.2–0.4 eV, and the lowest unoccupied molecular orbital of O_2 is higher than the Fermi level of the Al(111) surface, which is responsible for the barrier of the O_2 adsorption. Florian Libisch *et al.*[18] also investigated the origin of the energy barrier for chemical reactions of O_2 on Al(111). The results show that correct barriers arise naturally when embedded correlated electron wave functions are used to capture the physics of the interaction of O_2 with the metal surface. They suggested that the barrier originates from an abrupt charge transfer.

There are also many papers that have investigated the adsorption and desorption kinetics of water on aluminum,[19,20] the geometric, electronic and vibrational structure of the adsorbed layer,[19,21,22] and the oxidation kinetics of aluminum with water.[23,24] The adsorbed form of H_2O is predominantly molecular on the clean surface at low temperature, and in the presence of oxygen, the adsorbed form is predominantly

[a] Corrosion and Protection Center, Key Laboratory for Corrosion and Protection (MOE), University of Science and Technology Beijing, Beijing 100083, China. E-mail: cfdong@ustb.edu.cn; Fax: +86-10-62334005; Tel: +86-10-62333931 ext. 518

[b] School of Mathematics and Physics, University of Science and Technology Beijing, Beijing, 100083, China

dissociated. The production of adsorbed hydroxyl species from water reaches a maximum at 250 K on the clean surface and 350 K on a surface with pre-adsorbed O atoms.[25] A study by Paul and Hoffman showed that H_2O decomposed preferentially to surface-bound hydroxyl species. They also found that H_2O reversibly adsorbed on the Al(100) surface *via* hydrogen bonding, or H_2O dissociated into H and OH species.[26] Guo *et al.*[27] studied the energy barriers for the water dissociation processes using the nudge elastic band method. The results showed that hydrogen atom dissociation from H_2O requires 248.32 kJ mol^{-1} of energy on a clean Al(111) surface, whereas the dissociating energy decreased to 128.53 kJ mol^{-1} with the aid of O adsorption.

An accurate atomistic description of the H_2O-solid interface is crucial for understanding the oxidation mechanism of Al. Although scanning probe techniques, specifically scanning tunneling microscope, have contributed significantly to the field by providing detailed insight into the structure and dynamics of H_2O-adsorbed structures at the nanoscale, such studies are limited to well-defined, single crystal metal surfaces at low temperature and under ultra-high vacuum conditions. Computer calculation techniques, specifically density functional theory (DFT), have played a central role in understanding the mechanism of the interaction of H_2O with metal surfaces,[28] whereas these calculation remain an important problem. This is mainly because the standard DFT fails to describe the non-local van der Waals (vdW) dispersion forces, which are related to H_2O adsorption and weak adsorption systems in general.[28,29] As the problem exposed, a number of developments with DFT based schemes for dealing with vdW dispersion forces have been proposed.[30] The H_2O adsorption structures have been considered using dispersion-corrected DFT.[31–34] Indeed, the studies have indicated that vdW dispersion forces should be accounted for when describing the interaction between a H_2O molecule and a metal surface.

Here, we report a standard DFT study of the molecular and dissociative adsorptions of O_2 on a clean Al(111) surface. We use a vdW-DFT method to investigate the molecular adsorption of the H_2O on clean and oxygen pre-adsorbed Al(111) surfaces. The dissociation adsorption of H_2O molecule, that is, the co-adsorption of OH and H, was calculated using standard DFT after dispersion force testing. We analyze the structural evolutions, adsorption energies, charge transfer and partial density of states (PDOS) of the adsorbed structures and discuss the impact of the pre-adsorbed O atom on the H_2O adsorption behavior.

2. Computational details

2.1 Adsorption calculation

All calculations presented in this work were conducted using MedeA-VASP 5.4 software,[35,36] which is a fast and highly reliable electronic structure method that is based on DFT.[37] The calculation was conducted in a plane-wave basis, using the projector-augmented wave method.[38] The exchange–correlation functional for describing the interactions was GGA-PBE.[39] The adsorption calculations were conducted on 6-layer slabs of

Al(111) with a 12 Å vacuum gap. A (3×3) mesh was used for the adsorption calculation. The adsorbates and the three upper-most surface layers were allowed to move freely, and the bottom three layers were fixed. The electronic iterations convergence was 10^{-5} eV using the Normal (blocked Davidson) algorithm. Periodic boundary conditions were set, leading to an infinite periodic system.

The adsorption energies (E_{ad}) were calculated from the following expression:

$$E_{ad} = E_{ads} + E_{sub} - E_{ads/sub} \tag{1}$$

where E_{ads}, E_{sub} and $E_{ads/sub}$ represent the total energy of the isolated adsorbate, the relaxed clean slab and the slab covered with adsorbates, respectively. According to this definition, a larger adsorption energy means a stronger interaction between adsorbates and the substrate.

The surface energy (γ_{surf}) was calculated from the following expression:

$$\gamma_{surf} = (E_{sub} - nE_{atom-bulk})/2A \tag{2}$$

where E_{sub} is the total energy of the surface, $E_{atom-bulk}$ is the energy of a single Al atoms in bulk, n is the number of atoms of the slab surface, and A is the surface area.

All calculations involving O_2 were performed with a spin polarization to adequately describe the triplet state of O_2. Tests were established when the vdW dispersion force was considered for the molecular and dissociated adsorption of H_2O on the clean and O pre-adsorbed Al(111) surface. Based on previous calculations,[40] accounting for vdW dispersion forces does not change the adsorption structures. Table 1 shows the change of adsorption energy before and after considering non-local vdW dispersion forces. Comparing the DFT calculation with the vdW-DFT calculation in terms of adsorption energies, the vdW dispersion forces have a significant effect on the molecular adsorption of H_2O on the clean and oxygen pre-adsorbed Al(111) surface. Therefore, the vdW-DFT approximately takes into account the dispersive forces and vdW interactions in the molecular adsorption of H_2O. The optimized vdW functional based on the Becke 86 (optB86-vdW[41,42]), was chosen as the exchange functional, which tends to exhibit the smallest errors for most of the systems investigated. The non-local vdW correlation was not defined for a spin polarized system. The slab models were calculated using a ($4 \times 4 \times 1$)

Table 1 Effect of vdW dispersion force on the adsorption energy of the molecular and dissociated H_2O adsorbed structures

Adsorbed structure	Adsorption energy (eV)		
	DFT	vdW-DFT	$\Delta E/E_{ads\text{-}DFT}$ (%)
H_2O(top)	0.224	0.398	77.7
O(fcc)–H_2O(top)–O(fcc)	0.454	0.668	47.1
OH(fcc)–H(top)	7.539	7.728	2.5
OH(fcc)–OH(fcc)–O(fcc)	6.859	6.979	1.7

Monkhorst–Pack grid.[43] All calculations were performed using a 520 eV cut off energy. The post-processing of the results, which was based on structure and charge density, was constructed using VESTA.[44]

The so-called Bader scheme for dividing the slab surface into atomic regions has been used,[45] which proved to be robust and efficient. Included in MedeA-VASP as a property module, this approach is based on a classic algorithm, which was proposed by Bader and, implemented by Henkelman *et al.*[46] The calculation of difference charge density between the self-consistent pseudo charge density and the superposition of atomic charge densities is one of the most significant applications of pseudopotential theory. The property of PDOS was calculated to investigate the interaction between different atoms. From the PDOS diagram, the peak shifting indicates that the electronic number of the atom within a certain energy interval changed. The interaction between different atoms may relate to the overlapping of peaks.

2.2 Transition states search calculations

For the transition states search (TSS) calculation, the Nudged elastic band[47] method was used to map the minimum energy path between the initial system and the final system at a spring constant of 5 eV Å^{-2}. The initial images were created from linear interpolation. Reaction coordinate is the normalized coefficient of linear interpolation. Transition states (TS) were searched for the highest saddle point only. Optimization of transition states was attempted. The image closest to a saddle point was allowed to climb up into the saddle point if the largest force on an atom was smaller than 0.5 eV Å^{-1}. The SCF of each iteration was started from wave functions of the previous iteration. The convergence was 0.05 eV Å^{-1}. Diagonal elements of the inverse Hessian were initially set to 0.01 Å^2 eV^{-1}. The TSS calculation used normal precision and a plane wave cutoff energy of 520 eV. The electronic iterations convergence was 10^{-5} eV using the Normal (blocked Davidson) algorithm and reciprocal space projection operators. The K point was $4 \times 4 \times 1$. The vdW dispersion correction is considered for the TSS of the dissociation of H_2O.

3. Results and discussion

3.1 O atoms adsorption on the clean Al(111) surface

The calculated surface energy and work function of a clean six-layer Al(111) surface are 1.06 J m^{-2} and 4.12 eV, respectively, which agree well with corresponding experimental values of 1.14 J m^{-2} (ref. 48) and 4.24 eV,[49] respectively. Four highly symmetric adsorption sites were considered: top site, bridge site, fcc site and hcp site, as shown in Fig. 1. The O atoms could only adsorb on three hollow sites which are the fcc site and hcp site at coverages of 1/9 and 2/9 ML in our study. The adsorbed structures are listed in Table 2 and marked in Fig. 1. The geometrical parameters, adsorption energies and charge transfer details are provided in Table 2. For the single O atom adsorption, O(fcc1) and O(hcp1) structures were investigated. A chemical adsorption was observed, which was due to the close distance of Al–O (1.87 Å) and which is smaller than the sum of their ionic radii. The adsorption energy of the O(fcc1) structure is larger than that of O(hcp1) indicating a more stable adsorption, whereas the charge prefers to transfer to an O atom adsorbed on a hcp site. For the O adsorption on surface at coverages of 2/9 ML, six adsorbed structures were investigated, in which the O atoms were adsorbed on the fcc site and hcp sites at the nearest and next nearest adjacent distances. The adsorbed structures, geometrical parameters, adsorption energies and charge transfer details are shown in Table 2. The adsorption energies were calculated as the single O atom, which are basically consistent with previous calculations.[50] O(fcc1)–O(fcc2) is the most stable adsorbed structure of all the calculated structures at coverages of 2/9 ML according to the adsorption energies.

To further understand the mechanism of the O atom adsorption on the Al(111) surfaces, TSS calculations of the O atom along Al(111) surface and O pre-adsorbed Al(111) surface were calculated. The fcc site is the most stable site, and hcp is the metastable site of single O atom on the clean Al(111) surface. The hcp–fcc diffusion pathways of O atom on the clean and O(fcc) pre-adsorbed Al(111) surfaces were calculated. As shown in Fig. 2 and 3, energy barrier of 25.91 kJ mol^{-1} for the O
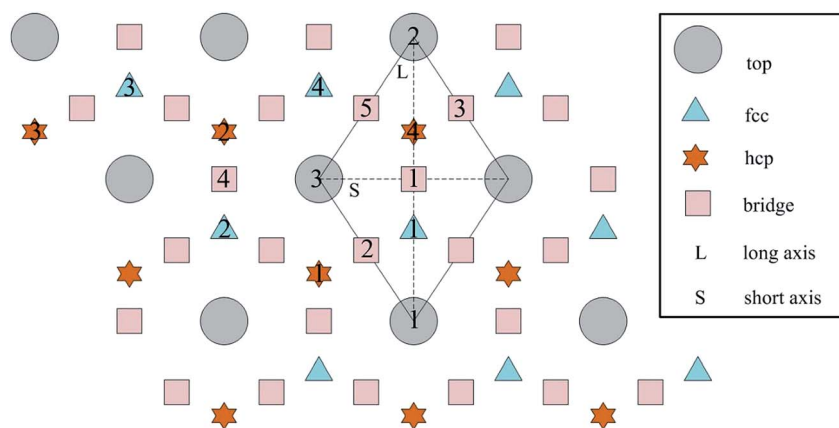

Fig. 1 The high symmetrical adsorption sites on the Al(111) surface.

Table 2 Geometrical parameters, adsorption energies and charge transfer of adsorbed structures of O atoms at the coverage of 1/9 ML and 2/9 ML on clean Al(111) surfaces

Adsorbed structure	Distance (Å)			Adsorption energy (eV)	Charge transfer	
	Al–O(fcc)	Al–O(hcp)	O–O		Al → O(fcc)	Al → O(hcp)
O(fcc1)	1.87	—	—	7.52	1.730	—
O(hcp)	—	1.87	—	7.21	—	1.759
O(fcc1)–O(fcc2)	1.86(1.86)	—	2.88	7.61	1.723(1.721)	—
O(fcc1)–O(fcc3)	1.86(1.87)	—	4.96	7.49	1.737(1.731)	—
O(fcc1)–O(hcp1)	1.85	1.86	2.39	7.22	1.686	1.711
O(fcc1)–O(hcp2)	186	1.87	3.32	7.40	1.734	1.763
O(hcp1)–O(hcp2)	—	1.86(1.87)	2.87	7.30	—	1.745(1.744)
O(hcp1)–O(hcp3)	—	1.87(1.86)	4.96	7.14	—	1.753(1.771)

diffusion on the clean surface is lightly lower than the corresponding values of 28.67 kJ mol^{-1} for the O diffusion on the O(fcc) pre-adsorbed Al(111) surface, suggesting that the adsorbed O atom on the fcc site slightly inhibits the diffusion of O atom on the Al(111) surface. The initial and final structures and their TS structures are also shown in Fig. 2 and 3, respectively. The bridge site is the adsorption site of the TS for both the clean surface and for the O(fcc) pre-adsorbed Al(111) surface.

3.2 Molecular adsorption of H$_2$O on Al(111) surfaces

3.2.1 H$_2$O adsorption on the clean Al(111) surface. The study by Netzer and Madey[19] showed that H$_2$O adsorbs on a top site on the Al(111) surface *via* an O atom, and the H$_2$O plane is almost parallel to the Al surface. Therefore, we mainly investigate two adsorbed adsorption structures with the O atom on a top site, H atoms on bridge sites and H–H line parallel to short axis and long axis, respectively. The adsorbed structures are labeled as H$_2$O(top3)–S and H$_2$O(top3)–L in Table 3. H$_2$O adsorbed on the surface in molecular form with O atoms closest to and H atoms furthest from the surface, which is in agreement with previous calculations. The geometric parameters, adsorption energy and charge transfer details are shown in Table 4,

which are basically the same for the two structures. The distance between the Al of the surface and O of H$_2$O is 2.15 Å in the two adsorbed structures, which is larger than the sum of their ionic radii. The average distance between H atoms and the O atom is 0.98 Å, which is slightly larger than that of 0.97 Å in H$_2$O vapor. The H–O–H internal angle is expanded by 0.1–0.2° from a calculated gas phase value of 104.6°. Both the adsorption energies and charge transfers from the surface to the H$_2$O molecule are very small. Thus, the interaction between H$_2$O and Al(111) is likely weak because of the long distance of Al–O, small deformation in H$_2$O, small adsorption energies and small charge transfer. To further illustrate the electronic interactions between H$_2$O and the Al(111) surface, we calculated the PDOS of the Al and O atom of the adsorbed structure, H$_2$O(top3)–S, and the results are provided in Fig. 4a. The resonance of the PDOS peaks of O(p) and Al(p) of the H$_2$O(top3)–S adsorbed structure occurs over the entire energy range, indicating that an interaction occurs between the Al atom of the surface and an O atom of H$_2$O.

3.2.2 H$_2$O adsorption on the O pre-adsorbed Al(111) surface. To investigate the effect of pre-adsorbed O atoms on the adsorption of H$_2$O on Al surface, two adsorbed structures with
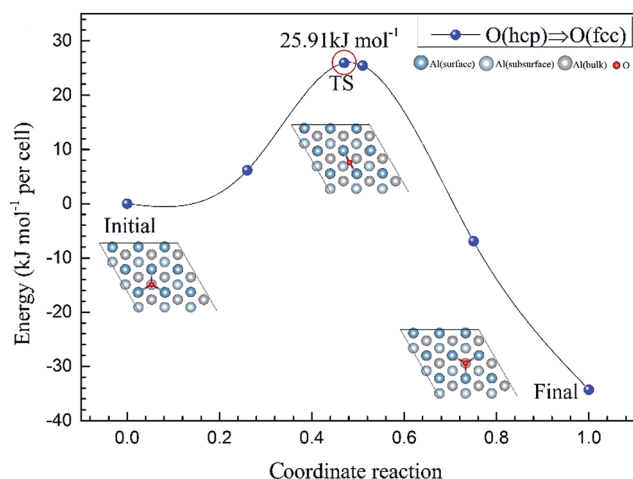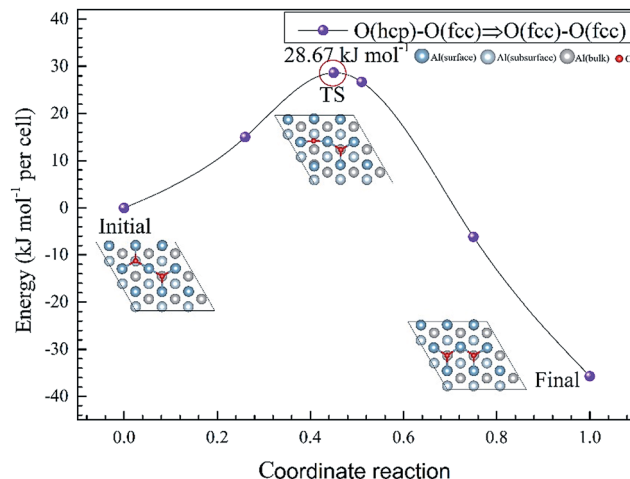

Fig. 2 The TSS results of single O atom along O(hcp)–O(fcc) pathway on the clean Al(111) surface.

Fig. 3 The TSS results of single O atom along O(hcp)–O(fcc) pathway on the O(fcc) pre-adsorbed Al(111) surface.

Table 3 Adsorbed structures of H_2O on the clean and oxygen pre-adsorbed Al(111) surfaces

Adsorbed structure	Top view	Side view
H_2O(top)–S		
H_2O(top)–L		
O(fcc)–H_2O(top)–O(fcc)–S		
O(fcc)–H_2O(top)–O(fcc)–L		
Remarks	Al(surface) Al(subsurface) Al(bulk) O H	

H_2O molecules that were close to pre-adsorbed O atoms were calculated. The adsorbed structures were also shown in Table 3. The O atoms pre-adsorbs on the fcc1 and fcc2 sites at a coverage of 2/9 ML, and H_2O adsorbs on the top site with the H–H line parallel to the short or long axis. The adsorbed structures are labeled as O(fcc1)–H_2O(top3)–O(fcc2)–S and O(fcc1)–H_2O(top3)–O(fcc2)–L. The geometric parameters, adsorption energies and charge transfer details were also shown in Table 4.

Additionally, H_2O adsorbs *via* the O atom on the top site in molecular form and the molecular deformation (bond length of H–O and bond angle of ∠HOH) is small with respect to gas phase H_2O. However, it is slightly larger than that on clean surface for all structures. The distances between the Al and O atom of H_2O decrease to 2.04 Å and 2.03 Å, which are almost equal to the sum of their ironic radii. The adsorption energies for H_2O adsorption on the O pre-adsorbed surface are obviously

Table 4 Geometrical parameters, adsorption energies and charge transfer of adsorbed structures of H_2O on the clean and oxygen pre-adsorbed Al(111) surfaces

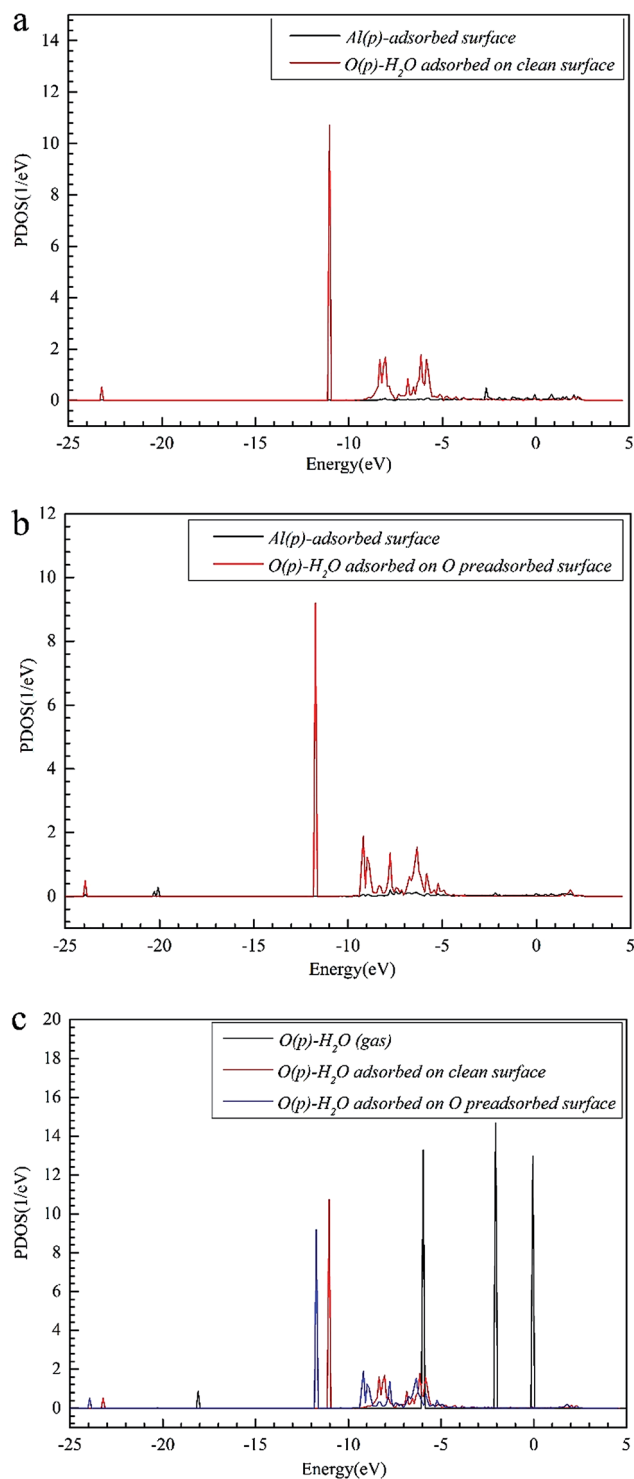| Adsorbed structure	Distance (Å)		∠HOH (°)	Adsorption energy (eV)	Charge transfer
	Al–O	H–O			
H_2O(top3)–S	2.15	0.98	106.2	0.398	0.079
H_2O(top3)–L	2.15	0.98	106.4	0.398	0.085
O(fcc1)–H_2O(top3)–O(fcc2)–S	2.04	0.98	106.7	0.668	0.004
O(fcc1)–H_2O(top3)–O(fcc2)–L	2.03	0.98	107.0	0.677	0.032

Fig. 4 The PDOS results of (a) Al(p) of the clean Al(111) surface and O(p) of H_2O adsorbed on the clean Al(111) surface; (b) Al(p) of the clean Al(111) surface and O(p) of H_2O adsorbed on the O pre-adsorbed Al(111) surface; (c) O(p) of H_2O in gas, H_2O adsorbed on the clean Al(111) surface, and H_2O adsorbed on the O pre-adsorbed surface.

surface significantly relative to that on the clean surface. Thus, the repulsive force between the O atom of H_2O and O atoms that are pre-adsorbed on surface may cause the Al atom to lie outside the surface.

The closer distance of Al–O and larger adsorption energies indicate a stronger adsorption for the H_2O on the O pre-adsorbed surface. The reduced charge transfer occurs because some of the electrons on the surface are controlled by the pre-adsorbed O atoms, which have a high electronegativity. The PDOS of Al(p) of surface and O(p) of the H_2O molecule was calculated for the O(fcc1)–H_2O(top3)–O(fcc2)–S structure shown in Fig. 4b. Similarly, the resonance of the PDOS peaks of O(p) and Al(p) of O(fcc1)–H_2O(top3)–O(fcc2)–S adsorbed structure occurs over the entire energy range. Fig. 4c shows the PDOS of O(p) of H_2O in gas, H_2O adsorbed on the clean surface and H_2O adsorbed on the O pre-adsorbed surface. The downshift of the O(p) state with respect to the gas is characterized by the displacement of the peak. The results illustrate that the adsorption of H_2O on the O pre-adsorbed surface is stronger adsorption on the clean surface, which agrees well with the conclusion inferred from geometrical parameters and adsorption results.

3.3 The dissociated adsorption of H_2O on Al(111)

We discuss the dissociated adsorption behavior of H_2O, that is, the co-adsorption of H and OH on the clean and O pre-adsorbed Al(111) surfaces. In total 17 initial and final structures of OH and H co-adsorbed on the clean Al(111) surface were investigated, which are listed in Table 5. The initial and final structures were characterized as shown in Fig. 1. The H atom can be adsorbed on the top2, top3, fcc2, and bridge1 sites when OH adsorbs on the top1 site and it migrates from bridge4 to fcc2 and hcp4 to bridge 1 sites, respectively. For the adsorption of OH on the fcc1 site, the H atom can adsorb on top2, and fcc2 directly and migrates from hcp4 to top3, and bridge4 to fcc2. The OH will migrate to the nearest bridge site when its initial site is hcp corresponding to H atom of different adsorbed sites. The geometrical parameters, adsorption energies and charge transfer details of OH and H co-adsorbed structures on clean Al(111) surface is shown in Table 5. There are chemical bonds between HO–Al and H–Al according to their distance and all structures have larger adsorption energies. The charge transfer from the surface to OH and H is much larger than the adsorption of H_2O molecule. Therefore, offering enough charge to H_2O is one of the necessary conditions to cause it to dissociate. Table 6 shows three possible adsorbed structures of OH and O on O(fcc1)–O(fcc2) pre-adsorbed Al(111) surfaces. The H atom that dissociated from H_2O bonds with one of two pre-adsorbed O atoms and adsorb on the surface in the form of OH. The geometrical parameters, adsorption energies and charge transfer details are shown in Table 7. Comparing with the adsorption of OH and H on the clean surface, both the adsorption energies and charge transfer of the adsorption on O pre-adsorbed surface decrease. Thus, the dissociated H_2O prefers to adsorb on a clean surface rather than on the O pre-adsorb surface, whereas the required charge transferred to

larger than on a clean surface, whereas the charge transfer decreases. For the adsorption of H_2O on O pre-adsorbed surface, the Al atom bonded to H_2O is pulled out of the

Table 5 Geometrical parameters, adsorption energies and charge transfer of OH and H dissociated from H_2O on the clean Al(111) surface

Initial structures	Adsorbed structures	Distance (Å)			E_{ads} (eV)	Charge transfer
		Al–O	Al–H	H–O		
OH(top1)–H(top2)	OH(top1)–H(top2)–L	1.74	1.62	0.97	7.14	1.412
OH(top1)–H(top3)	OH(top1)–H(top3)–S	1.74	1.62	0.97	7.12	1.421
OH(top1)–H(fcc2)	OH(top1)–H(fcc2)	1.75	1.92	0.97	7.28	1.705
OH(top1)–H(bridge4)	OH(top1)–H(fcc2)	1.75	1.92	0.97	7.28	1.701
OH(top1)–H(hcp4)	OH(top1)–H(bridge1)	1.73	1.81	0.98	7.19	1.689
OH(fcc1)–H(top2)	OH(fcc1)–H(top2)	2.07	1.63	0.98	7.33	1.638
OH(fcc1)–H(fcc2)	OH(fcc1)–H(fcc2)	2.07	1.92	0.98	7.45	1.891
OH(fcc1)–H(hcp4)	OH(fcc1)–H(top3)	2.05	1.62	0.98	7.39	1.636
OH(fcc1)–H(bridge4)	OH(fcc1)–H(fcc2)	2.07	1.63	0.98	7.45	1.890
OH(hcp4)–H(top1)	OH(bridge1)–H(top1)	1.90	1.66	1.01	7.54	1.629
OH(hcp4)–H(fcc2)	OH(bridge1)–H(fcc2)	1.94	1.91	0.98	7.44	1.854
OH(hcp4)–H(hcp1)	OH(bridge1)–H(hcp1)	1.94	1.91	0.98	7.25	1.868
OH(hcp4)–H(bridge4)	OH(bridge5)–H(bridge4)	1.93	1.74	0.98	7.34	1.783
OH(bridge2)–H(top2)	OH(bridge2)–H(top2)	1.94	1.62	0.98	7.31	1.570
OH(bridge2)–H(fcc4)	OH(bridge2)–H(fcc4)	1.95	1.92	0.98	7.45	1.846
OH(bridge2)–H(hcp4)	OH(bridge2)–H(bridge3)	1.93	1.83	0.98	7.41	1.756
OH(bridge2)–H(bridge5)	OH(bridge2)–H(fcc4)	1.94	1.92	0.98	7.45	1.851

H_2O that adsorbed on O pre-adsorbed surface was significantly reduced.

To elucidate the mechanisms of the dehydrogenated reaction of single H_2O on the clean and O pre-adsorbed surfaces, the energy barriers for the H_2O dissociation processes were calculated using the TSS method. The energy barriers and structural evolution of the systems for H_2O dissociation on the clean and O pre-adsorbed Al(111) surfaces are shown in Fig. 5 and 6. There is a high energy barrier for H_2O dissociation on the clean surface. For the case of H_2O dissociation on the O pre-

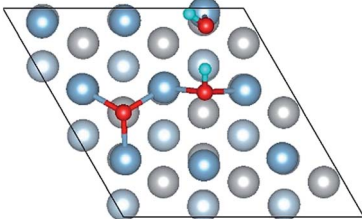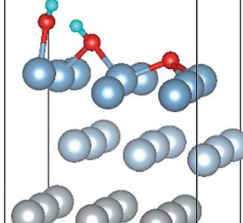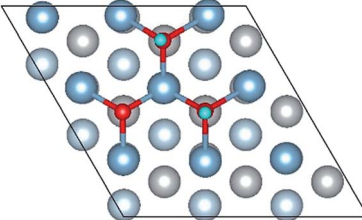**Table 6** Dissociated adsorbed structures of H_2O on the O pre-adsorbed Al(111) surface
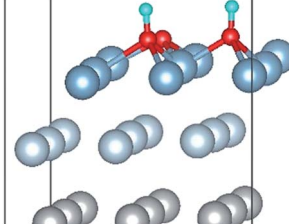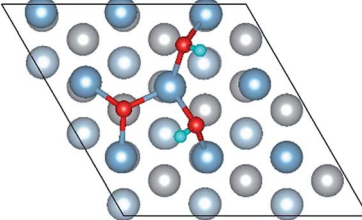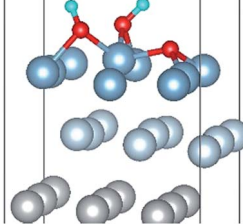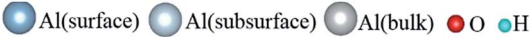
Adsorbed structure	Top view	Side view
OH(bridge1)–OH(top2)–O(fcc2)		
OH(fcc1)–OH(fcc4)–O(fcc2)		
OH(bridge2)–OH(bridge5)–O(fcc2)		
Remarks		

⬤ Al(surface) ◯ Al(subsurface) ◯ Al(bulk) ● O ● H

Table 7 Geometrical parameters, adsorption energies and charge transfer of OH and H dissociated from H_2O on the oxygen pre-adsorbed Al(111) surface

Adsorbed structure	Distance (Å)			E_{ads} (eV)	Charge transfer
	Al–O(fcc)	Al–O(OH)	O–H		
OH(bridge1)–OH(top2)–O(fcc2)	1.86	1.86	1.00	6.87	0.330
OH(fcc1)–OH(fcc4)–O(fcc2)	1.87	2.06	0.98	6.85	0.375
OH(bridge2)–OH(bridge5)–O(fcc2)	1.86	1.92	0.98	6.76	0.311
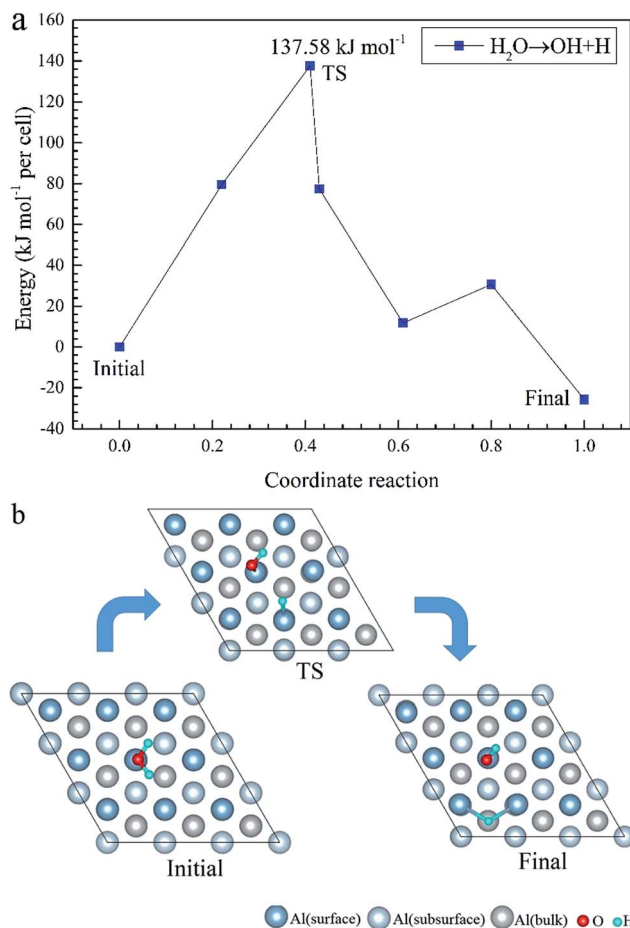
Fig. 5 The TSS results of dissociated reaction of H_2O molecule on the clean Al(111) surface.
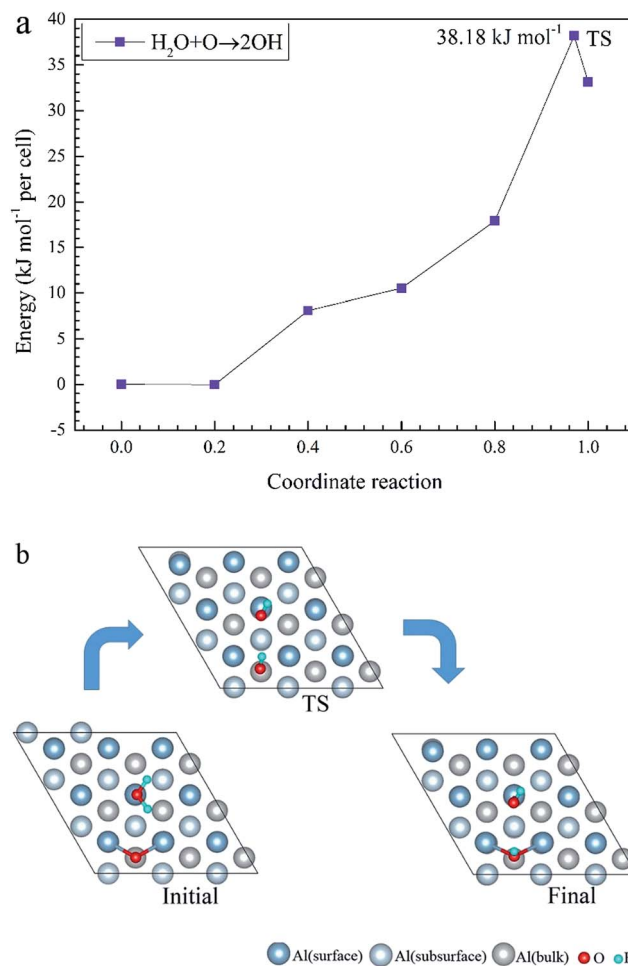
Fig. 6 The TSS results of dissociated reaction of H_2O molecule on the O(fcc) pre-adsorbed Al(111) surface.

adsorbed surface, the dissociation energy barrier reduced significantly compared with that on clean surface, which indicates that the active energy of H_2O dissociation decreased due to the pre-adsorbed O atom. Upon comparison of the energy of the initial and final adsorbed structures, the dissociation of H_2O on the clean surface was found to be spontaneous reaction with a high energy barrier. However, the dissociation of H_2O on the O pre-adsorbed surface is a non-spontaneous process with a low active energy barrier. The pre-adsorbed O is an electronegative atom that makes it more attractive than Al for the H atom of H_2O. When O adsorbs on the Al(111) surface, the electrons of Al are attracted toward the O atom. Therefore, the

pre-adsorbed O will weaken the O–H bond and cause it easily dissociate.

4. Conclusions

Using first-principles calculations that are based on DFT, the molecular and dissociative adsorptions of O_2 and H_2O on clean and oxygen pre-adsorbed Al(111) surfaces were investigated. The adsorbed structures, adsorption energy, PDOS, charge transfer from surface to the adsorbates and energy barriers for O atom migration and H_2O dissociation are calculated. The main conclusions are summarized as follows:

(1) For the adsorption of O_2 on the clean Al(111) surface, O_2 dissociates into O atoms which can adsorb on the fcc and hcp sites of the clean Al(111) surface, and the ranking of adsorption site stability was found to be fcc > hcp. The energy barriers for a single O atom along the hcp–bridge–fcc pathway on the clean and O(fcc) pre-adsorbed Al(111) surface are 25.91 kJ mol^{-1} and 28.67 kJ mol^{-1} indicating that the pre-adsorbed O atom has a weak inhibiting effect on O atom migration.

(2) H_2O can only adsorb in the form of a molecule on both the clean and O pre-adsorbed Al(111) surfaces, and the adsorption is very weak. The PDOS results show that the pre-adsorbed O atoms on the surface can strengthen the adsorption of H_2O and promote its deformation.

(3) The dissociation adsorption of H_2O, that is, the co-adsorption of OH and H, is much stronger than the molecular adsorption of H_2O. On the clean Al(111) surface, the dissociation of a single H atom from H_2O requires 137.58 kJ mol^{-1}. However, with the aid of the pre-adsorbed O atom, the dissociating energy decreases to 38.18 kJ mol^{-1}, suggesting that pre-adsorbed O can promote the dissociation of H_2O.

Acknowledgements

References

1 B. B. Wang, Z. Y. Wang, W. Han and W. Ke, *Corros. Sci.*, 2012, **55**, 63–70.

2 S. Sun, Q. Zheng, D. Li and J. Wen, *Corros. Sci.*, 2009, **51**, 719–727.

3 Y. Shi, Z. Zhang, J. Su, F. Cao and J. Zhang, *Corros. Sci.*, 2006, **51**, 4977–4986.

4 S. Sun, Q. Zheng, D. Li, S. Hu and J. Wen, *Corros. Sci.*, 2011, **53**, 2527–2538.

5 Y. L. Cheng, Z. Zhang, F. H. Cao, J. F. Li, J. Q. Zhang, J. M. Wang and C. N. Cao, *Corros. Sci.*, 2004, **46**, 1649–1667.

6 N. D. Alexopoulos, *Corros. Sci.*, 2012, **55**, 289–300.

7 S. Liu, H. Sun, L. Sun and H. Fan, *Corros. Sci.*, 2012, **65**, 520–527.

8 C. Leygraf and T. E. Graedel, *Atmospheric corrosion, electrochemical society series*, Wiley-interscience, 2000.

9 A. Pashutski, A. Hoffman and M. Folman, *Surf. Sci. Lett.*, 1989, **208**, L91–L97.

10 A. J. Komrowski, J. Z. Sexton, A. C. Kummel, M. Binetti, O. Weiße and E. Hasselbrink, *Phys. Rev. Lett.*, 2001, **87**, 246103.

11 H. Brune, J. Wintterlin, R. J. Behm and G. Ertl, *Phys. Rev. Lett.*, 1992, **68**, 624.

12 X. Lei and L. Yang, *Comp. Appl. Chem.*, 2011, **28**, 793–796.

13 D. Costa, T. Ribeiro and F. Mercuri, *Adv. Mater. Interfaces*, 2014, **1**, 1300072.

14 M. Shao, Y. Fu, R. Hu and C. Lin, *Mater. Sci. Eng., A*, 2003, **344**, 323–327.

15 X. Liu, G. S. Frankel, B. Zoofan and S. I. Rokhlin, *Corros. Sci.*, 2007, **49**, 139–148.

16 B. C. Mitrovic and D. J. O'Connor, *Surf. Sci.*, 1998, **405**, 261–270.

17 H.-R. Liu, H. Xiang and X. G. Gong, *J. Chem. Phys.*, 2011, **135**, 214702.

18 J. Carrasco, J. Klimeš and A. Michaelides, *Phys. Rev. Lett.*, 2013, **138**, 024708.

19 F. P. Netzer and T. E. Madey, *Surf. Sci.*, 1983, **127**, L102–L109.

20 U. Memmert, S. J. Bushby and P. R. Norton, *Surf. Sci.*, 1989, **219**, 327–340.

21 J. E. Crowell, J. G. Chen, D. M. Hercules and J. T. Yates Jr, *J. Chem. Phys.*, 1987, **86**, 5804–5815.

22 P. B. Smith and S. L. Bernasek, *J. Electron Spectrosc. Relat. Phenom.*, 1989, **49**, 149–158.

23 F. Szalkowski, *J. Chem. Phys.*, 1982, **77**, 5224–5227.

24 H. D. Ebinger and J. T. Yates Jr, *Surf. Sci.*, 1998, **412/413**, 1–11.

25 J. E. Crowell, J. G. Chen, D. M. Hercules and J. T. Yates Jr, *J. Chem. Phys.*, 1987, **86**, 5804–5815.

26 J. Paul and F. M. Hoffman, *J. Phys. Chem.*, 1986, **90**, 5321–5324.

27 F. Y. Guo, C. G. Long, J. Zhang, Z. Zhang, C. H. Liu and K. Yu, *Appl. Surf. Sci.*, 2015, **324**, 584–589.

28 J. Carrasco, A. Hodgson and A. Michaelides, *Nat. Mater.*, 2012, **11**, 667–674.

29 A. Hodgson and S. Haq, *Surf. Sci. Rep.*, 2009, **64**, 381–451.

30 J. Klimeš and A. Michaelides, *J. Chem. Phys.*, 2012, **137**, 120901.

31 I. Hamada, K. Lee and Y. Morikawa, *Phys. Rev. B: Condens. Matter Mater. Phys.*, 2010, **81**, 115452.

32 T. Kumagai, H. Okuyama, S. Hatta, T. Aruga and I. Hamada, *J. Chem. Phys.*, 2011, **134**, 024703.

33 A. Poissier, S. Ganeshan and M. V. Fernández-Serra, *Phys. Chem. Chem. Phys.*, 2011, **13**, 3375–3384.

34 K. Tonigold and A. Gross, *J. Comput. Chem.*, 2012, **33**, 695–701.

35 G. Kresse and J. Hafner, *Phys. Rev. Lett.*, 1993, **47**, 558–561.

36 G. Kresse and J. Furthmüller, *J. Phys. Chem. B*, 1996, **54**, 11169–11186.

37 W. Kohn and L. J. Sham, *Phys. Rev. A*, 1965, **140**, 1133–1138.

38 G. Kresse and D. Joubert, *Phys. Rev. B: Condens. Matter Mater. Phys.*, 1999, **59**, 1758–1775.

39 J. P. Perdew, K. Burke and M. Ernzerhof, *Phys. Rev. Lett.*, 1996, **77**, 3865–3868.

40 F. A. Soria, P. Paredes-Olivera and E. M. Patrito, *J. Phys. Chem. C*, 2015, **119**, 284–295.

41 J. Klimeš, D. R. Bowler and A. Michaelides, *Phys. Rev. B: Condens. Matter Mater. Phys.*, 2011, **83**, 195131.

42 J. Klimeš, D. R. Bowler and A. Michaelides, *J. Phys.: Condens. Matter*, 2010, 22022201.

43 H. Monkhorst and J. Pack, *Phys. Rev. B: Condens. Matter Mater. Phys.*, 1976, **13**, 5188–5192.

44 K. Momma and F. Izumi, *J. Appl. Crystallogr.*, 2008, **41**, 653–658.

45 R. F. W. Bader, *Atoms in Molecules-A Quantum Theory*, Oxford University Press, New York, 1990.

46 G. Henkelman, A. Arnaldsson and H. Jónsson, *Comput. Mater. Sci.*, 2006, **36**, 354–360.

47 J. Henkelman and H. J. Jonsson, *Chem. Phys.*, 2000, **113**, 9978–9985.

48 W. R. Tyson and W. A. Miller, *Surf. Sci.*, 1977, **62**, 267–276.

49 H. B. Michaelson, *J. Appl. Phys.*, 1977, **48**, 4729–4733.

50 A. Kiejna and B. I. Lundqvist, *Phys. Rev. B: Condens. Matter Mater. Phys.*, 2011, **83**, 085405.